# Formation of drug-loaded nanoemulsions in stirred media mills

Julia Felicitas Schwendner, Christoph Konnerth, Stefan Romeis, Jochen Schmidt[*], Wolfgang Peukert

Institute of Particle Technology (LFG), Friedrich-Alexander-Universität Erlangen-Nürnberg (FAU), Cauerstraße 4, 91058 Erlangen, Germany


[*] Author to whom the correspondence should be addressed:

Dr. Jochen Schmidt

Institute of Particle Technology (LFG),

Cauerstraße 4, 91058 Erlangen, Germany

Phone: +49 9131 / 8529408

Fax: +49 9131 / 8529402

E-Mail: jochen.schmidt@fau.de


Authors email address:

julia.schwendner@fau.de (J. Schwendner), christoph.konnerth@fau.de (C. Konnerth) stefan.romeis@fau.de (S. Romeis), jochen.schmidt@fau.de (J. Schmidt), wolfgang.peukert@fau.de (W. Peukert)

**Highlights**

- Nanoemulsions with drug-loaded oil phases are produced in stirred media mills.

- Approach is demonstrated for model active pharmaceutical ingredients dissolved in plant oils.

- Influence of surfactant-to-oil-weight-ratio on droplet size is studied.

- *In vitro* study of drug distribution.

**Abstract**

The feasibility of stirred media mills for the production of nanoemulsions loaded with active pharmaceutical ingredients (API) using plant oils as disperse phase and different types of the non-ionic emulsifier polysorbate is demonstrated. The influence of the emulsion formulation, namely oil type, surfactant and surfactant-to-oil-weight-ratio (SOR) on the product droplet size at constant stressing conditions is studied in detail. At similar stressing conditions and SOR, the type of the used plant oil and surfactant did not influence the product droplet size and the smallest achievable median droplet size was 20 nm. The API saturated oil phases and the pure oil phases exhibit similar viscosities, emulsification kinetics and final product droplet sizes, i.e. no influence of the API on the emulsification process could be identified. However, a strong dependency of the emulsion droplet size on the SOR has been observed. Moreover, very good long-term stabilities could be achieved for the obtained emulsions. A release test with fenofibrate-loaded peanut oil-polysorbate 80-water nanoemulsions showed remarkably fast drug distribution as compared to a formulation containing the same amount of the non-dissolved micronized drug.

# 1.    Introduction

Emulsions are colloidal dispersions with droplet sizes in the range between a few 10 nanometers and several hundreds of microns [1,2]. The most common types of emulsions are microemulsions and nanoemulsions, which fundamentally differ in terms of thermodynamic stability [3,4]. Microemulsions form spontaneously and are thermodynamic stable. Typically very high emulsifier concentrations (>20 %) are required [5]. In contrast, nanoemulsions are thermodynamically unstable colloidal systems and exhibit only kinetic stability. Compared to microemulsions, the droplet formation in nanoemulsions does not occur spontaneously, i.e. a high energy input is needed to rupture large droplets into smaller ones during the emulsification process [6].

Nanoemulsions as colloidal delivery systems for lipophilic bioactive ingredients are of increasing interest, especially in the pharmaceutical, cosmetic and food industry [6–9]. In recent years, the incorporation of a variety of poorly water-soluble active pharmaceutical ingredients (APIs), flavouring agents, nutrients, nutraceuticals, carotenoids, essential oils and vitamins has been successfully achieved [2,10,11].

Nanoemulsions exhibit a high loading capacity for hydrophobic substances in combination with their ability to protect drugs from hydrolysis and enzymatic degradation [4]. Thus, the formation of nanoemulsions is a promising formulation strategy to overcome poor solubility and bioavailability issues [4]. Examples for commercial parenteral nanoemulsions are Diprivan®, Limethason®, Ropivon® and Vitalipid® [12]. Moreover, nanoemulsions show improved dermal and transdermal drug permeability [5,13]. Furthermore, compared to conventional drug application forms (e.g. capsules, drug suspensions) a significant increase of relative bioavailability and permeability parameters, such as the steady state flux and the

4

permeability coefficient could be observed for nanoemulsion formulations of poorly soluble APIs [13–15].

A broad variety of production methods for nanoscale emulsion systems has been proposed so far. In high energy emulsification processes droplet break-up occurs due to forces exerted on the dispersed phase by the continuous phase. These forces are induced by shear and elongation stress in laminar or turbulent flow regimes.

High energy emulsification processes which rely on the application of external energy include high pressure homogenizers, rotor-stator devices, orifices, membranes and porous media [8,16–24]. In addition to the aforementioned high energy production methods, low energy techniques, such as phase inversion methods and self-emulsifying drug delivery systems (SEDDS) are frequently used for the production of emulsions [5,11,25–28]. For the latter, however, the use of co-surfactants, synthetic surfactants and in most cases very high surfactant concentrations are a considerable disadvantage with respect to pharmaceutical and food applications.

Schmidt et al. successfully applied emulsification in stirred media mills for the production of n-alkane-polysorbate 85-water nanoemulsions with volume median droplet diameters between 10 and 100 nm and narrow size distributions [29]. It could be shown that -besides the surfactant-to-oil-mass-ratio (SOR = $m_{surfactant}$ : $m_{oil}$)- the applied stressing conditions (c.f. stress energy and stress number [30]) strongly affect the emulsification result [29]. It was found that applying small grinding bead diameters $d_{GM}$ and high stirrer tip speeds $v_{tip}$ is advantageous with respect to fast process kinetics, small droplet sizes and a narrow width of the droplet size distribution. Based on these findings, all experiments in the present study were performed using beads with a nominal diameter $d_{GM}$ = 100 µm at a maximum stirrer tip speed $v_{tip}$ = 6.7 m/s, corresponding to the maximum tip speed in the used batch mill.

Emulsification experiments with different plant oils were performed and compared to a mineral oil system. Different types of nonionic polysorbate emulsifiers, varying in molecular weight and hydrophilic-lipophilic balance (HLB), were applied to stabilize the nanoemulsions. In particular, the influence of type and SOR on emulsification kinetics and final product droplet size as well as the influence of type and concentration of dissolved drug were studied. Long-term stability of the oil-polysorbate-water-formulations has been observed for almost over two months. Moreover, a release study of the API is presented. It was found, that API-loaded nanoemulsions produced by stirred media emulsification exhibit a considerably fast drug distribution in a defined release medium as compared to micronized API particles.

## 2.    Materials and methods

### 2.1.    Materials

Peanut oil, sesame oil and soy bean oil (Henry Lamotte Oils, Germany), as well as the mineral oil n-hexadecane (> 95 %, for synthesis, Alfa Aesar, Germany) have been used as oil phases in the emulsification experiments. All plant oils are refined and meet the requirements according to the European Pharmacopoeia. Different polysorbates were applied as non-ionic emulsifiers. Polyoxyethylene (20) sorbitan monolaurate (polysorbate 20) and polyoxyethylene (20) sorbitan monooleate (polysorbate 80) were purchased from Merck (Germany), Polyoxyethylene (20) sorbitan monopalmitate (polysorbate 40), and polyoxyethylen (20) sorbitan trioleate (polysorbate 85) from Sigma Aldrich (Germany). Deionized water produced by the Millipore device Purelab Ultra (Veolia Water, France) was used as continuous phase. The APIs fenofibrate (≥ 99 %, Sigma Aldrich, Germany) and ibuprofen (> 98.0 %, TCI EUROPE N.V., Belgium) have been dissolved in the respective oil phases. All chemicals were used without further purification.

### 2.2.    Methods

#### 2.2.1.    Emulsification process

Emulsification experiments have been performed using the vertical laboratory stirred media mill PE075 (Netzsch Feinmahltechnik, Germany) equipped with a double-walled grinding chamber for temperature control and an $Al_2O_3$ three-disc-stirrer. The temperature in the process chamber has been adjusted to $(20 \pm 1.5)$ °C using the thermostat FPW80-SL (Julabo, Germany). Approximately 1900 g of wear resistant yttrium-stabilized zirconium oxide beads (YTZ®, $\rho_{GM}$ of 6050 kg/m³, Tosoh, Japan) with a nominal diameter $d_{GM}$ of 100 µm were filled into the grinding chamber. The stirrer tip speed $v_{tip}$ has been set to 6.7 m/s. The aforementioned stressing conditions

were used in all experiments presented in the following. Oil mass fractions $m_{oil}$ up to 15 wt.% and emulsifier mass fractions $m_{surfactant}$ ranging from 1.0 to 5.0 wt.% with respect to the total mass have been applied. First, the emulsifier was completely dissolved under stirring in the aqueous phase and the organic compound was completely dissolved in the oil phase by ultrasonic treatment. The aqueous emulsifier solution and the oil phase, in total 200 mL, were subsequently transferred to the grinding chamber and the emulsification process was started. Samples for droplet size analyses were taken at fixed process times from the middle of the grinding bead bed. Further information is given in [29].

For comparison, emulsification has been performed by a rotor-stator device ultra-turrax T18 basic (IKA-Werke, Germany) as well. An oil mass fraction $m_{oil}$ of 5 wt.% and an emulsifier mass fraction $m_{surfactant}$ of 5.0 wt.% with respect to the total mass applied in the stirred media emulsification experiments. The ultra-turrax has been operated at 10000 rpm for a process time of 180 min at (20 ± 2) °C controlled by a tempered water bath.

### 2.2.2.  Droplet size analysis

Droplet size distributions were determined by dynamic light scattering (DLS) using a Honeywell Ultrafine Particle Analyzer 150 (UPA, Microtrac, USA). To avoid multiple scattering, all samples were diluted with deionized water by a factor of about 12 inside the measuring chamber. The size measurements have been performed at (20 ± 1.5) °C. In the following, average values and calculated standard deviations obtained from six single measurements are reported.

### 2.2.3.  Viscosity measurements

Oil viscosity was determined using a MCR 302 rotational rheometer (Anton Paar GmbH, Austria) in double gap configuration at $(20 \pm 0.2)$ °C. Flow curves were measured for shear rates between 10 s$^{-1}$ and 1000 s$^{-1}$. All measurements were performed in triplicate.

### 2.2.4.  *In vitro* release study

*In vitro* studies regarding drug distribution were performed using the USP apparatus II VK7000 (Vankel Technology Group, USA). The paddle rotation was set to 75 rpm and the temperature was kept constant at $(37 \pm 0.5)$ °C using the VK 750D external heater circulator (Vankel Technology Group, USA). Hard gelatine capsules (Size 0, Wepa Apothekenbedarf, Germany) were filled either with 0.5 mL of emulsion or 1.4 mg of drug particles: Both formulations contained the same amount of the API. As release medium 900 mL of deionized water with 0.94 mM polysorbate 80 was used. Sink conditions during the release study were assured by the presence of polysorbate 80, which increases the API saturation solubility as compared to pure water [31] remarkably, c.f. Supplementary Figure S1. Sample aliquots of 0.5 mL were filtered through a 0.2 µm syringe filter with cellulose acetate membrane (VWR International, Germany) for removal of drug particles or any other possible particles. The filtered samples were subsequently transferred and sealed in 1.5 mL vials (VWR International, USA) for HPLC analysis (see section 2.2.5). After sampling, an equal volume of fresh dissolution medium was added to maintain a constant volume in the system. Three independent dissolution experiments were performed.

## 2.2.5. High performance liquid chromatography

Fenofibrate was quantitatively determined by high performance liquid chromatography (HPLC). The used HPLC device (Thermo Fisher Scientific) was equipped with a quaternary analytical pump LPG-3400SD, an automated sample injector ASI-100, a column thermostat STH 585 and a diode array detector DAD-3000RS. The chromatographic column UltraSep ES AMID H RP18 (column size 150x3 mm, SEPSERV Separation Service, Germany) was used for separation at 25 °C. The mobile phase was composed of acetonitrile (ROTISOLV® HPLC Gradient Grade, Carl Roth, Germany) and water (70:30 (v/v)) and the flow rate was 0.5 mL/min. Fenofibrate was detected at a wavelength of 285 nm. The retention time was 4 min 30 s under the aforementioned conditions. The limit of detection of fenofibrate calculated from the calibration graph was 0.039 mg/L. All experiments were performed in triplicate.

## 3. Results and discussion

### 3.1. Influence of oil type on droplet size

Emulsification experiments with the three different biocompatible plant oils (peanut oil, sesame oil, soy bean oil) were performed under identical process conditions (mentioned in section 2.2.1) and were compared to the mineral oil system. Emulsification kinetics for the plant oils and the n-hexadecane in presence of the non-ionic surfactant polysorbate 85 are given in Figure 1. As can be seen, the temporal evolution of the volume median droplet size $x_{50,3}$ for the investigated emulsion systems at constant SOR (5:5), constant stressing conditions and temperature is similar: With increasing process time, a decrease in droplet size (and span ($(x_{90,3} - x_{10,3}) / x_{50,3}$), c.f. Figure 3) is observed. A stationary minimum median droplet diameter $x_{50,3}$ lower than 50 nm is found for process times exceeding approx. 130 minutes. Emulsions produced with n-hexadecane as oil phase exhibit smaller droplet sizes as compared to the plant oils, which can be explained by lower viscosity ratio $\eta_D / \eta_C$ ($\eta_D$: dispersed phase viscosity, $\eta_C$: viscosity of the continuous phase) for the hexadecane system (c.f. a lower critical capillary number $Ca_{crit}$ for droplet rupture) which leads to an 'easier', respectively more efficient droplet break-up.
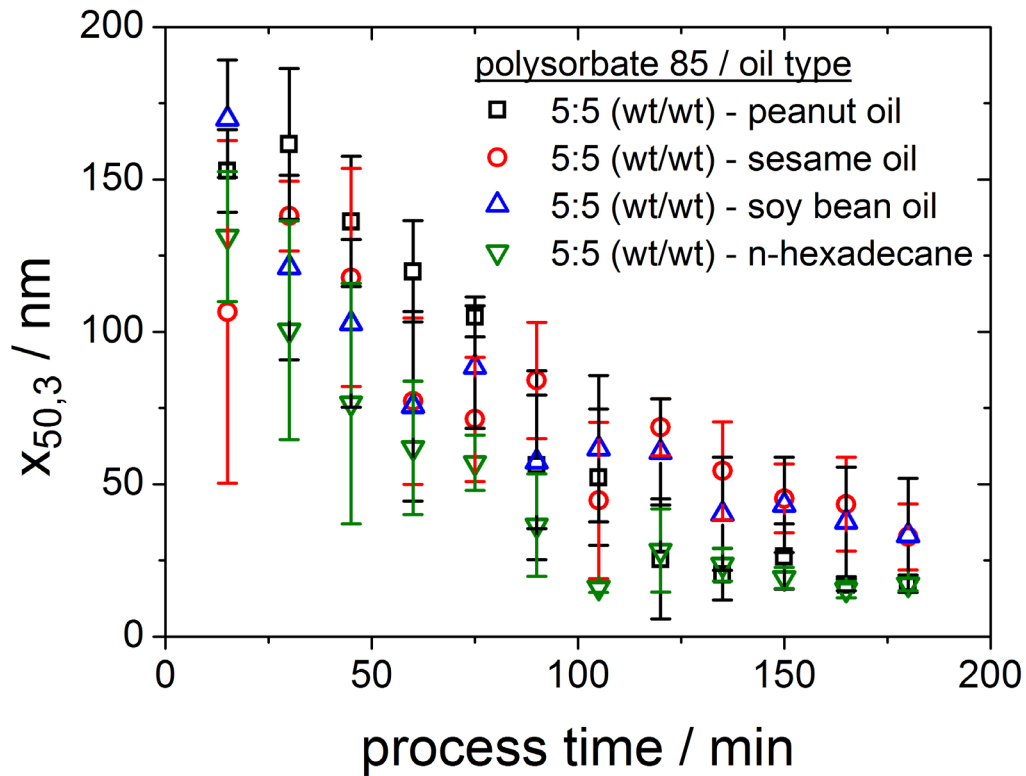
**Figure 1** *Influence of oil type on the evolution of the volume median diameter $x_{50,3}$ of an oil-polysorbate 85-water-system during processing at constant SOR (5:5), stressing conditions ($d_{GM}$ = 100 µm, $v_{tip}$ = 6.7 m/s) and process temperature ($T_{process}$ = 20 °C).*

**Table 1** *Viscosity of oil phases and viscosity ratios $\eta_D$ / $\eta_C$ for the emulsion systems.*

| Type | $\eta$ (1000 s$^{-1}$, 20 °C) mPas | $\eta_D$ / $\eta_C$ (1000 s$^{-1}$, 20 °C) |
|---|---|---|
| water | 0.96 ± 0.01 | - |
| n-hexadecane | 6.52 ± 0.09 | 6.79 |
| peanut oil | 81.00 ± 0.06 | 84.38 |
| sesame oil | 70.20 ± 0.06 | 72.92 |
| soy bean oil | 62.23 ± 0.05 | 64.58 |

Wooster et al. [32] reported that the formation of small droplets is most efficient when using low oil phase viscosities $\eta_D$ or rather low dispersed / continuous phase viscosity ratios ($\eta_D / \eta_C$). In case of the n-hexadecane-polysorbate 85-system, a comparatively small viscosity ratio applies, see Table 1. According to literature [2,32–34], the optimum range, where droplet break-up is most effective, is $0.1 < \eta_D / \eta_C < 5$. Droplet break-up takes place in extensional shear flow and in laminar shear flow. For viscosity ratios $\eta_D / \eta_C > 4$ droplet break-up only occurs in extensional shear flow because the critical capillary number $Ca_{critical}$ and the influence of the viscosity ratio is much smaller than in laminar shear flow [2,35,36]. With respect to the ratio of $\eta_D / \eta_C$ (c.f. Table 1) droplet break-up is easier for the n-hexadecane system. No remarkable influence of the viscosity on droplet formation is observable when comparing the plant oils, see Figure 1. Furthermore, the composition of the plant oils with respect to the varying amounts of different fatty acids like the ratio of oleic acid and linoleic acid did not significantly influence the emulsification process for the investigated formulations and SOR. Thus, in summary no influence of the plant oil type on the emulsification process was found.

## 3.2. Influence of emulsifier type on droplet size

The influence of the emulsifier type on the volume median diameter $x_{50,3}$ of the product emulsion obtained for a peanut oil-polysorbate-water-system was investigated for four different polysorbates, namely polysorbate 20, polysorbate 40, polysorbate 80 and polysorbate 85. The aforementioned emulsifiers differ in constitution with respect to the type (length) of the fatty acid tails. Key physicochemical properties of the used polysorbate types are summarized in Table 2. All used polysorbates exhibit a HLB suitable to produce oil-in-water (O/W) emulsions

[2,6]. All applied emulsifier concentrations clearly exceed the corresponding critical micelle concentration (CMC) values.

**Table 2** *Characteristics of applied polysorbates.*

| Type | Molecular weight[a] g / mol | HLB[a] | CMC[b] g / 100 mL (25 °C) |
|---|---|---|---|
| Polysorbate 20 | 1228 | 16.7 | 0.0060 |
| Polysorbate 40 | 1284 | 15.6 | 0.0031 |
| Polysorbate 80 | 1310 | 15.0 | 0.0014 |
| Polysorbate 85 | 1838 | 11.0 | 0.0023 |

[a] [37] [b] [38]

The theoretical obtainable minimum droplet size can be estimated from equation (1) [39]. Here, monolayer coverage of the droplet surface with surfactant molecules is assumed.

$$x_{1,2,min} = \frac{6\varphi}{1000 A_{surfactant} N_A} \frac{1}{\frac{c_{surfactant}}{M_{surfactant}} - CMC(1-\varphi)} \tag{1}$$

The minimum possible droplet size is expressed by the minimum Sauter diameter $x_{1,2,min}$. CMC corresponds to the critical micelle concentration (mol/L), $\varphi$ is the disperse phase volume fraction, $A_{surfactant}$ is the area occupied by one emulsifier molecule at the liquid-liquid interface (m²), $c_{surfactant}$ is the emulsifier concentration

(g/L), $N_A$ is the Avogadro number (1/mol) and $M_{surfactant}$ is the molar mass of the emulsifier (g/mol).

The minimum droplet size estimated according to eq. 1 is mainly determined by the value assumed for the interfacial area occupied by an emulsifier molecule, $A_{surfactant}$. Data on the occupied interfacial area for one emulsifier molecule are scarce; for polysorbate 80 a value of 2.48 $nm^2$ was reported [40]. For the other polysorbates no data were available, moreover, $A_{surfactant}$ will not only depend on the constitution of the surfactant and the type of interface but also on other system parameters like temperature, pH, ionic strength, affinity of the emulsifier to the oil phase and the aqueous phase. To account for the uncertainty of $A_{surfactant}$ and to exemplify the influence on this quantity on the estimated $x_{1,2min}$, $A_{surfactant}$ has been varied in a reasonable range and values of 1 $nm^2$, 2 $nm^2$, 2.48 $nm^2$ [40] and 3 $nm^2$ have been assumed. The calculated estimates for $x_{1,2min}$ are summarized in Table 3 for a SOR of 5:5: Irrespective of the assumed value of $A_{surfactant}$ the estimate and the experimentally observed minimum droplet Sauter diameter $x_{1,2}$ at the most vary by an order of magnitude:

**Table 3** *Comparison of estimates for $x_{1,2min}$ according to eq. 1 under variation of the surface area occupied by one emulsifier molecule $A_{surfactant}$ and the experimentally observed minimum droplet size $x_{1,2}$ for a SOR of 5:5.*

| $A_{surfactant}$ / $nm^2$ | 1.00 | 2.00 | 2.48 | 3.00 | |
|---|---|---|---|---|---|
| Type | $x_{1,2,min}$ / nm | $x_{1,2,min}$ / nm | $x_{1,2,min}$ / nm | $x_{1,2,min}$ / nm | $x_{1,2}$ / nm |
| Polysorbate 20 | 12.2 | 6.1 | 5.0 | 4.1 | 44 ± 8 |

| | | | | |
|---|---|---|---|---|
| Polysorbate 40 | 12.8 | 6.4 | 5.2 | 4.3 | 34 ±13 |
| Polysorbate 80 | 13.1 | 6.5 | 5.3 | 4.4 | 13 ± 2 |
| Polysorbate 85 | 18.3 | 9.2 | 7.4 | 6.1 | 20 ± 7 |

When assuming $A_{surfactant}$ = 2.48 nm$^2$, as reported by Haque et al. [40], the experimentally observed minimum droplet size $x_{1,2}$ for the polysorbate 80 system is 2.5 times larger than the estimated minimum droplet size $x_{1,2,min}$, c.f. Table 3. Fair agreement is observed. One has to take into account that, this estimation does not consider important coarsening phenomena such as droplet coalescence. Moreover, any limitations due to the distribution of the surfactant molecules in the oil and water phase are not implied within these considerations.
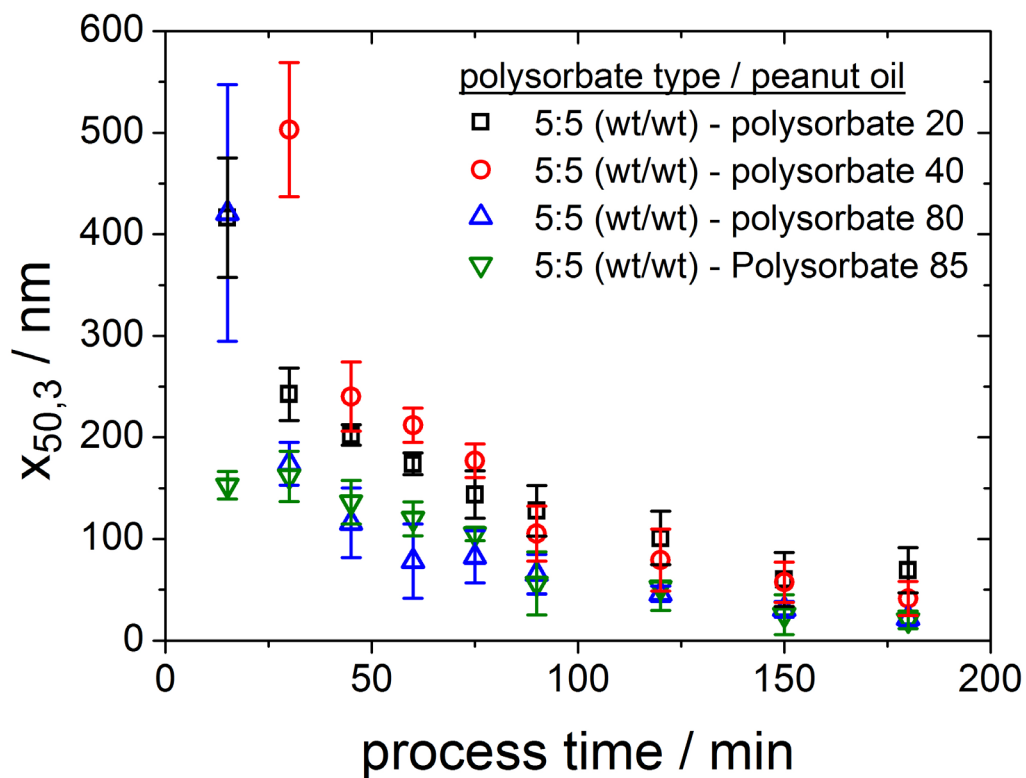


**Figure 2** *Influence of polysorbate type on the evolution of the volume median diameter $x_{50,3}$ of a peanut oil-polysorbate-water-system during processing at constant SOR (5:5), stressing conditions ($d_{GM}$ = 100 µm, $v_{tip}$ = 6.7 m/s) and process temperature ($T_{process}$ = 20 °C).*
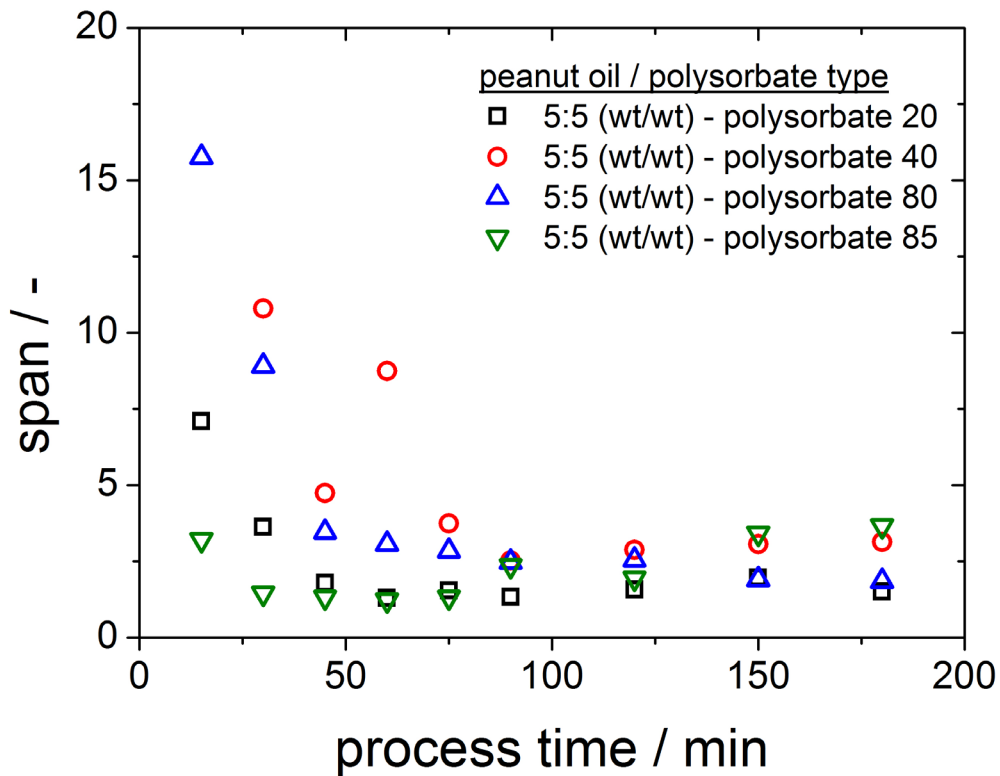
**Figure 3** *Influence of polysorbate type on the evolution of the span of a peanut oil-polysorbate-water-system during processing at constant SOR (5:5), stressing conditions ($d_{GM}$ = 100 µm, $v_{tip}$ = 6.7 m/s) and process temperature ($T_{process}$ = 20 °C).*

**Table 4** *Droplet sizes of peanut oil (5 wt.-%) – polysorbate (5 wt.-%) - water nanoemulsions after a process time of 180 minutes.*

| Type | $x_{10,3}$ / nm | $x_{50,3}$ / nm | $x_{90,3}$ / nm | $x_{1,2}$ / nm | span - |
|---|---|---|---|---|---|
| Polysorbate 20 | 45 ± 13 | 69 ± 22 | 156 ± 12 | 44 ± 8 | 1.6 |
| Polysorbate 40 | 25 ± 5 | 41 ± 17 | 143 ± 32 | 34 ± 13 | 2.8 |
| Polysorbate 80 | 14 ± 5 | 22 ± 7 | 51 ± 7 | 13 ± 2 | 1.7 |
| Polysorbate 85 | 12 ± 2 | 20 ± 8 | 70 ± 13 | 20 ± 7 | 2.5 |

Emulsification kinetics of a peanut oil-polysorbate-water-system at constant SOR of 5:5 show a similar trend of the evolution of the product droplet size over process time for different polysorbate types, see Figure 2. Obviously, the differences regarding the final volume median diameters $x_{50,3}$ of the emulsion systems are from around a few nanometers to 50 nm. The smallest oil droplets were obtained by applying polysorbate 85 ($x_{50,3} \approx 20$ nm) as emulsifier. In contrast, the usage of polysorbate 20 led to median droplet sizes $x_{50,3}$ of around 69 nm. As depicted in Figure 3, the evolution of the span is inversely proportional to the process time during the first 2 h. For longer process times, the spans slightly increase, which can be attributed to some coalescence. With respect to the key physicochemical properties of the used surfactants (see Table 2), no significant correlation between the molecular weights and the HLB values of the different polysorbate emulsifiers and the resulting droplet diameters can be deduced. Obviously, polysorbate 85 led to the smallest mean particle sizes and spans for short process times. However, this trend reversed for longer process times when slight coalescence sets in. The better stabilization with longer chains can be explained by steric effects, whereas the observed coalescence is surprising and, in particular with respect to long-term stability, needs further investigation.

Besides oil and emulsifier type also the influence of the SOR on the emulsification process was studied. Figure 4 displays the dependency of the volume median diameter $x_{50,3}$ on the SOR.
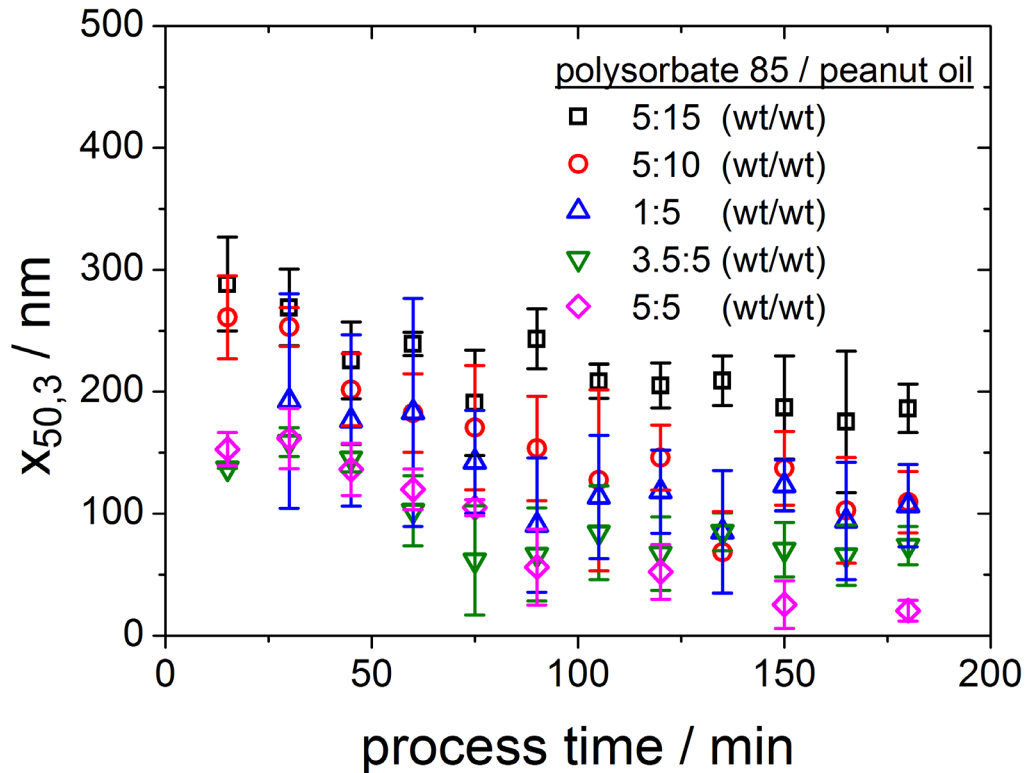
**Figure 4** *Influence of the SOR on the evolution of the volume median diameter $x_{50,3}$ of a peanut oil-polysorbate 85-water-system during processing at constant stressing conditions ($d_{GM}$ = 100 µm, $v_{tip}$ = 6.7 m/s) and process temperature ($T_{process}$ = 20 °C).*

The SOR was varied by increasing the amount of oil and keeping the amount of emulsifier constant and by changing the amount of surfactant at constant oil mass. As shown in Figure 4, only a slight decrease of the mean droplet diameter over process time could be observed with small amounts of surfactant and high oil concentrations (c.f. SOR = 1:5 / 5:15 / 5:10). Under the aforementioned conditions the amount of surfactant was not sufficient to stabilize the newly formed surface of the droplets adequately and droplet coalescence occurred. Moreover, viscosity effects prevent proper emulsification at high oil concentrations (15 / 10 wt.%). Higher oil contents lead to an increase of the viscosity of the continuous phase. Hence, the droplet break-up rate decreases remarkably [5,41–43]. Thus, if high oil

19

concentrations are applied, less efficient drop size reduction is observed. Moreover, the number of produced oil droplets increases with the oil content. Thus, the coalescence rate increases [2].

The fastest emulsification kinetics and the smallest volume median diameters $x_{50,3}$ were found for the highest SOR (5:5), where obviously sufficient surfactant molecules are present for an adequate and fast oil droplet stabilization. Higher surfactant concentrations in the continuous phase allow for rapid diffusion and adsorption of the surfactant molecules to the newly formed emulsion droplet surface [44–46]. In summary, the SOR influences the formation of nanoemulsions strongly, whereas the choice of the emulsifier type depends on the intended application of the emulsion (e.g. pharmaceutical, food or cosmetic emulsion).

## 3.3. Influence of drug load on droplet size

In the following, the influence of different model API loads on the observed droplet size $x_{50,3}$ was studied for emulsification of peanut oil, see Figure 5: The performance of the emulsification process using stirred media mills with respect to achievable minimum droplet sizes is obvious when comparing the emulsion systems to a processed micellar solution of the used emulsifier, i.e. a dispersion of micelles formed by the emulsifier in the aqueous system in the absence of the API-loaded oil phase. Characteristic physicochemical properties of the hydrophobic APIs are summarized in Table 5. For fenofibrate in pure water a saturation solubility of 0.36 mg/L (37 °C) was observed, which in good agreement with data from literature [31].
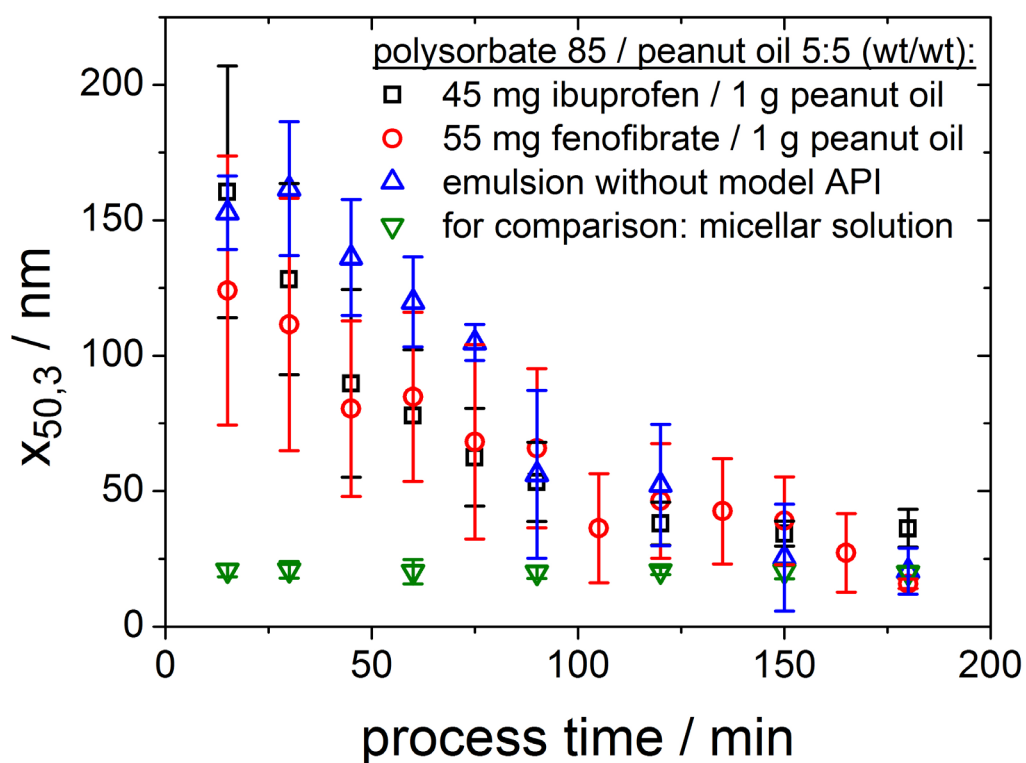
**Figure 5** *Influence of the drug load of different organic compounds on the evolution of the volume median diameter $x_{50,3}$ of an oil-polysorbate 85-water-system during processing at constant SOR (5:5), stressing conditions ($d_{GM}$ = 100 µm, $v_{tip}$ = 6.7 m/s) and process temperature ($T_{process}$ = 20 °C).*

**Table 5** *Physicochemical properties of organic compounds.*

| Organic compound | Molecular weight[a] g / mol | Log $P_{O/W}$ | $c_{sat.}$ (water) mg / L | $V_m$[d] cm$^3$ / mol | $c_{sat.}$ (peanut oil) mg / mL |
|---|---|---|---|---|---|
| Fenofibrate | 360.83 | 5.24[b] | 0.358 ± 0.003 (37°C)[g] | 311 | 47.5[e] |
| Ibuprofen | 206.28 | 3.24[c] | 49 ± 2 (25 °C)[c] | 200 | 48.5[f] |

[a] Manufacturers´ data. [b] [47] [c] [48] [d] [49] [e] [50] [f] [51] [g] Experimental data.

Almost identical temporal evolutions of the droplet diameters for oil phases loaded either with fenofibrate or ibuprofen have been observed during emulsification. After the same process times, similar droplet diameters were obtained, i.e. there is no pronounced influence of the organic load. No significant differences between the oil viscosity of the loaded and the pure oil phase were found (Table 6). Therefore, we conclude that the type of the drug load will not influence the obtained droplet sizes remarkably, if the viscosity of the saturated oil remains -more or less- unaffected by the drug in the oil phase.

**Table 6** *Viscosity of drug loaded peanut oil.*

| Type | $\eta$ (1000 s$^{-1}$, 20 °C) / mPas |
| --- | --- |
| Peanut oil | 81.00 ± 0.06 |
| Peanut oil + fenofibrate (10 mg / ml) | 81.70 ± 0.00 |
| Peanut oil + fenofibrate saturated | 86.70 ± 0.06 |
| Peanut oil + ibuprofen (10 mg / ml) | 83.40 ± 0.06 |
| Peanut oil + ibuprofen saturated | 86.30 ± 0.06 |

In summary, the emulsification process was found to be independent of the drug load for comparable systems. Consequently, the interfacial activity of the surfactant predominates the activity of the oil-dissolved hydrophobic organic compounds. Thus, the emulsifier (type and concentration) will mainly determine emulsion stability and (minimum) product droplet size.

### 3.4. Long-term stability of nanoemulsions

Besides small droplet sizes and narrow distributions, stability issues play an important role in the application. Therefore, the stability of the peanut oil-polysorbate 80-water-system and the polysorbate 85-water-system produced by media milling emulsification experiments was investigated. The emulsions were stored in the fridge at a temperature of (6 ± 2) °C for a period of approximately two months. Figure 6 depicts the evolution of the oil droplet diameter $x_{50,3}$ and the span for peanut oil-polysorbate-water-systems as a function of the storage time.
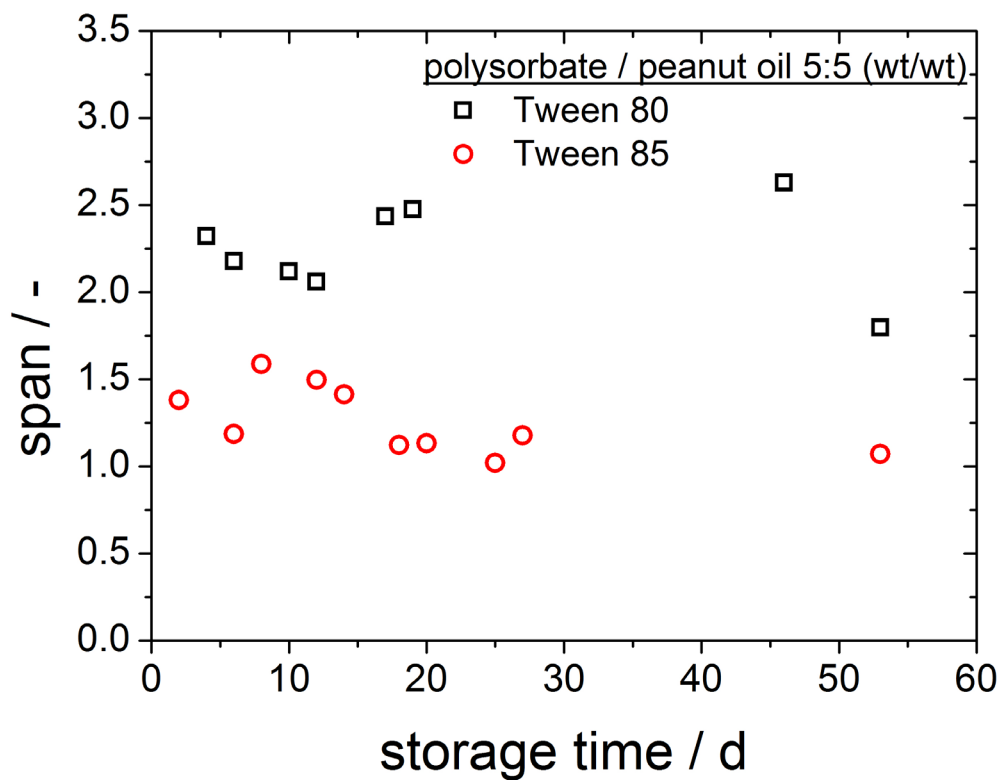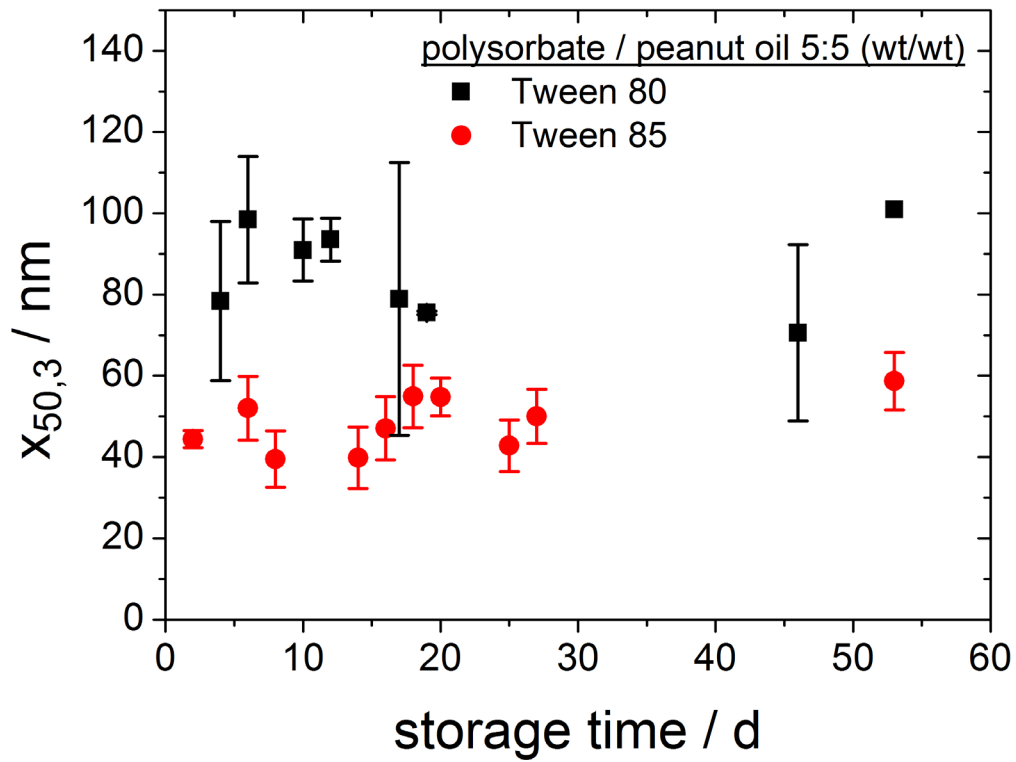
**Figure 6** *Evolution of (a) droplet diameters $x_{50,3}$ and (b) span of peanut oil-polysorbate-water-systems stored at (6 ± 2) °C.*

Both peanut oil-polysorbate-water-emulsions showed good long-term stability within the investigated time period of 53 days characterized by only minor changes of span and droplet size, see Figure 6. Moreover, in these systems no break-up or creaming was observed. Emulsion breakdown due to gravitational separation, like creaming and sedimentation is prevented due to the small droplet size of the nanoemulsions. Moreover, nanoemulsions show high stability against flocculation and coalescence because colloidal interactions are minimised with decreasing droplet size [1,5,10].

### 3.5. Comparison of stirred media milling and alternative emulsification processes

For high energy emulsification a variety of different devices are used, both in science and industry [8,19,20,23]. To compare the stirred media emulsification process with alternative approaches, nanoemulsions (at same SOR) have also been produced with a rotor-stator device. Figure 7 depicts the evolution of the droplet diameter $x_{50,3}$ as a function of the process time of the emulsification processes using a stirred media mill and an ultra-turrax stirrer, respectively. The evolution of the span over process time for the two emulsification methods is given, too. While the nanoemulsion produced with the stirred media mill is characterized by very small span values and rather constant droplet size readings during particle sizing (c.f. red square symbols in Figure 7a, small error bars), the product emulsions obtained with the ultra-turrax are instable which is reflected by the large scattering of the observed droplet sizes during sizing and very large spans. Thus, stirred media emulsification yields stable and narrowly distributed droplet sizes well below 50 nm (for a process time of 180 minutes), while emulsification using the rotor-stator device even for these quite long process time does not yield stable sub- 100nm product emulsions: During bead collisions in the stirred media mill elongational and shear flow situations are

induced in a highly parallelized manner leading to very efficient emulsification as expressed by the small and rather monodisperse droplets. Also emulsification by the ultra-turrax leads to almost identical mean particle sizes, however, the accompanying spans are significantly larger, which promotes coarsening phenomena: within a time period of eight days, droplet diameters roughly tripled and significant creaming was observed (data not shown).
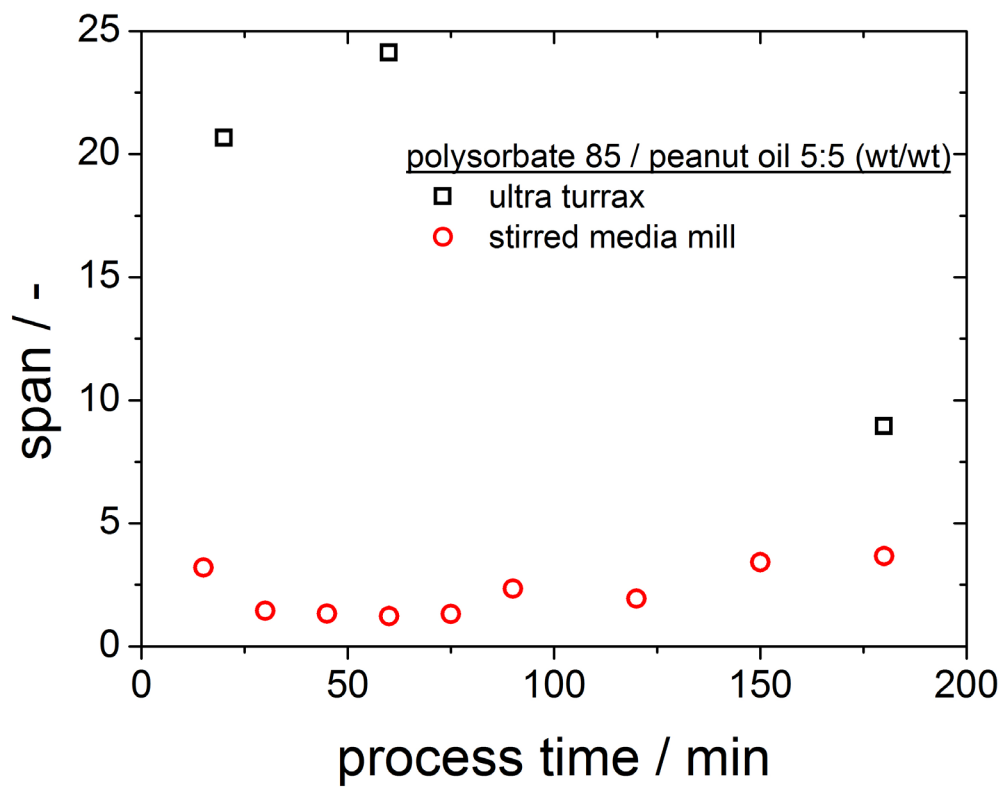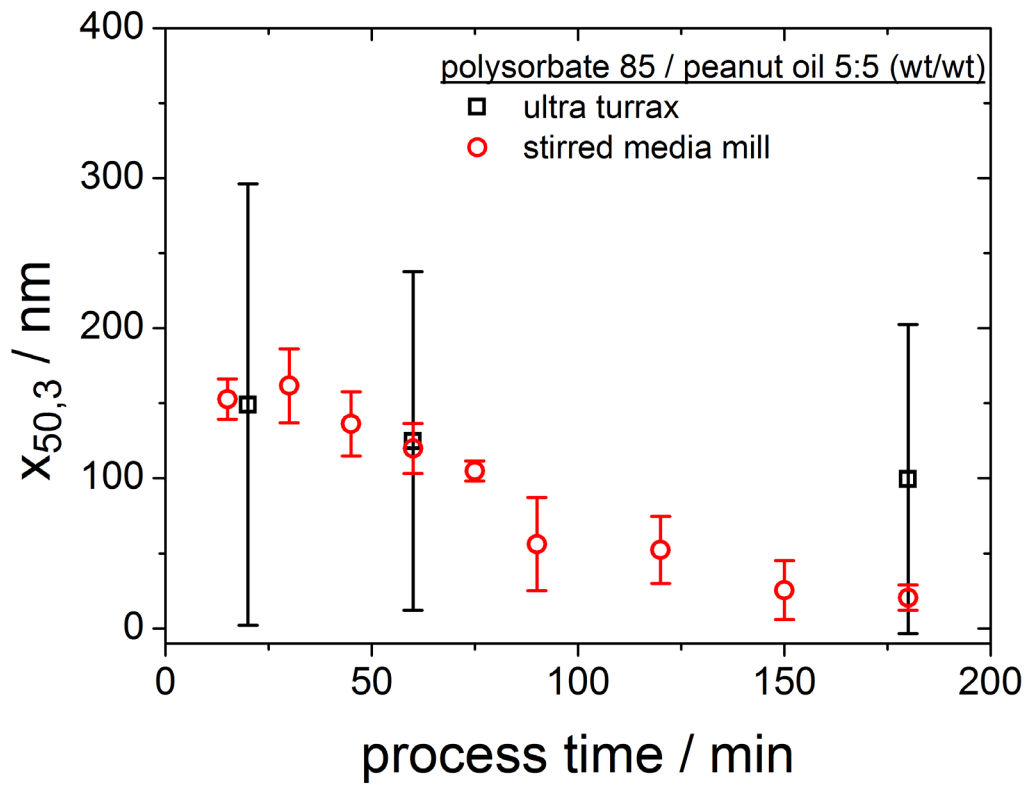
**Figure 7** *Comparison of the temporal evolution of (a) the volume median droplet diameter $x_{50,3}$ and (b) the span of the product emulsion for a peanut oil-*

*polysorbate 85-water-system 5:5 (wt/wt) emulsified with a stirred media mill and an ultra-turrax stirrer.*

## 3.6. Nanoemulsions as drug delivery systems

An *in vitro* release study using an USP II dissolution apparatus was performed under sink conditions to compare the temporal drug release from the API-loaded nanoemulsion system and micronsized fenofibrate, respectively. Sink conditions were assured by the addition of polysorbate 80 to the release medium: an increase of the saturation solubility of fenofibrate in the presence of micelle-forming species has been reported by Granero et al. [31] for sodium lauryl sulfate and was observed with polysorbate 80 as well (see Supplementary Figure S1): a remarkable increase of API solubility in the presence of polysorbate 80 as compared to pure water (c.f. Table 5) was found. The temporal evolution of released fenofibrate is summarized in Figure 8 using formulations containing $c_{drug} = 2.78$ mg/mL of API and 26.7 mM of polysorbate 80. In pharmaceutical formulations polysorbate 80 is more frequently used than polysorbate 85. Hence, the presented experiments were performed with polysorbate 80 as surfactant. The maximum theoretical concentration of fenofibrate detectable in the dissolution medium $V_{medium}$ of 900 ml after the application of the nanoemulsion and the drug particles in the gelatine capsules with the amount $V_{emulsion} = 0.5$ ml of emulsions was 1.54 mg/L (($c_{drug} \cdot V_{emulsion}$) / ($V_{medium} + V_{emulsion}$)).
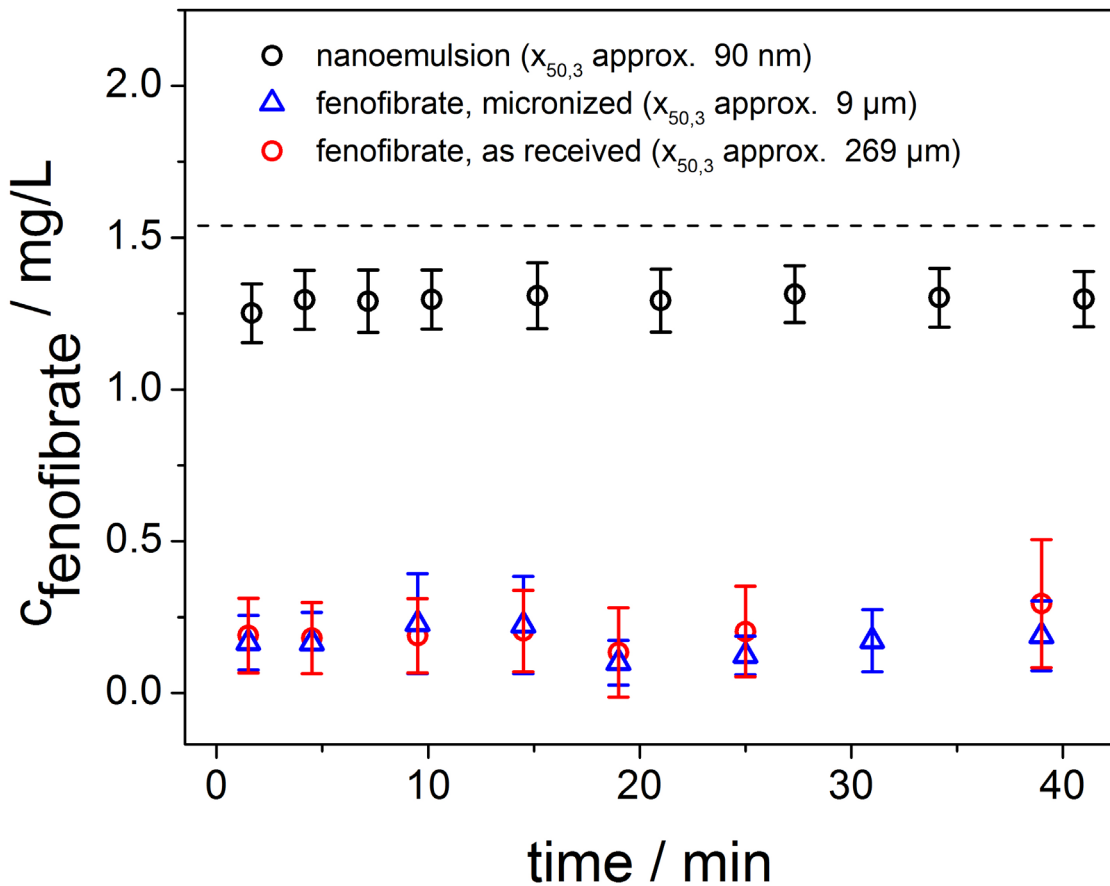
**Figure 8** *Fenofibrate supply of a loaded peanut oil-polysorbate 80-water-system and fenofibrate drug particles (as received and micronized) in an USP II dissolution apparatus (75 rpm, 37 °C). The maximum fenofibrate concentration possible in the release experiment is depicted by the black dotted line. Each formulation contained 2.78 mg/mL of API and 26.7 mM of polysorbate 80.*

As shown in Figure 8, in contrast to the fenofibrate dispersion systems, the nanoemulsion system provides instantaneous availability of the API due to efficient distribution of the drug in the release medium in the USP apparatus: roughly by a factor of 20 higher fenofibrate concentrations are available in the medium as compared to the release studies for micron-sized drug particles for the times

considered. For the nanoemulsion formulation around 95 % of the applied drug concentration could be detected after 60 min. From the drug particles only a very small amount of dissolved fenofibrate could be detected within the considered time period. All measured concentrations are within a narrow band at concentrations below 0.4 mg/L. The fenofibrate supply of the nanoemulsions occurred quasi-instantaneously at much higher concentrations.


## 4.      Conclusions

Emulsification in stirred media mills has been demonstrated as an appropriate method to produce API-loaded nanoemulsions using plant oil as dispersed phase and polysorbates as emulsifier. The product droplet size at constant stressing conditions is strongly dependent on the surfactant-to-oil-weight-ratio (SOR). At constant amount of emulsifier only slightly different final product droplet sizes are found for the different types of polysorbate. No systematic dependency with respect to constitution, HLB value or molecular weight could be identified.

The well-known influence of the viscosity ratio on droplet break-up [30-34] was confirmed for the stirred media emulsification as well: For plant oil emulsion systems (viscosity ratio $\eta_D / \eta_C$ between 65 to 87) larger minimum product droplet sizes as compared to a mineral oil (hexadecane) emulsion system ($\eta_D / \eta_C = 5$) were found. No influence of the type of the used plant oil on the product droplet size at same stressing conditions and same SOR was found. Moreover, API saturated oil phases and the pure oil phase showed similar viscosities, similar emulsification kinetics and final product droplet sizes. Obviously the API does not influence the emulsification process remarkably.

Moreover, long-term stability of the peanut oil-polysorbate 85 and polysorbate 80-water-systems for storage periods of up to 50 days was studied as the droplet

diameter influences considerably emulsion stability. Gravitational separation and droplet aggregation mechanism are minimised in nanoemulsions. *In vitro* release experiments using the USP II apparatus with nanoemulsions prepared from an oil phase containing fenofibrate showed that the nanoemulsion provides the API almost instantly to the dissolution medium due to the good distribution of the API nanoemulsion droplets. In contrast, the dissolution kinetics of the solid drug are comparatively slow. Thus, the production of API-loaded nanoemulsions prepared by stirred media emulsification is a feasible formulation strategy to overcome the challenge of poor solubility and, thus, poor bioavailability of many active pharmaceutical ingredients.

## 5.    Acknowledgments

## 6.    References

**References**

[1]  C. Solans, P. Izquierdo, J. Nolla, N. Azemar, M. Garcia-Celma, Nano-emulsions, Current Opinion in Colloid & Interface Science 10 (3-4) (2005) 102–110. https://doi.org/10.1016/j.cocis.2005.06.004.

[2]  H. Schubert, Emulgiertechnik: Grundlagen, Verfahren und Anwendungen, 2nd ed., Behr, Hamburg, 2010.

[3]  D.J. McClements, Nanoemulsions versus microemulsions: terminology, differences, and similarities, Soft Matter 8 (6) (2012) 1719. https://doi.org/10.1039/c2sm06903b.

[4]  C. Lovelyn, A.A. Attama, Current State of Nanoemulsions in Drug Delivery, JBNB 02 (05) (2011) 626–639. https://doi.org/10.4236/jbnb.2011.225075.

[5]  T. Tadros, P. Izquierdo, J. Esquena, C. Solans, Formation and stability of nano-emulsions, Adv Colloid Interface Sci 108-109 (2004) 303–318. https://doi.org/10.1016/j.cis.2003.10.023.

[6]  B.P. Binks, Modern Aspects of Emulsion Science, Royal Society of Chemistry, Cambridge, 1998.

[7]  H.P. Schuchmann, T. Danner, Emulgieren: Mehr als nur Zerkleinern, Chem-Ing-Tech 76 (4) (2004) 364–375. https://doi.org/10.1002/cite.200406163.

[8]  T.G. Mason, J.N. Wilking, K. Meleson, C.B. Chang, S.M. Graves, Nanoemulsions: formation, structure, and physical properties, J. Phys.: Condens. Matter 18 (41) (2006) R635-R666. https://doi.org/10.1088/0953-8984/18/41/R01.

[9]  M.N. Yukuyama, E.T.M. Kato, R. Lobenberg, N.A. Bou-Chacra, Challenges and Future Prospects of Nanoemulsion as a Drug Delivery System, Curr. Pharm. Des. 23 (3) (2017) 495–508. https://doi.org/10.2174/1381612822666161027111957.

[10] D.J. McClements, E.A. Decker, J. Weiss, Emulsion-based delivery systems for lipophilic bioactive components, J. Food Sci. 72 (8) (2007) R109-24. https://doi.org/10.1111/j.1750-3841.2007.00507.x.

[11] F. Ostertag, J. Weiss, D.J. McClements, Low-energy formation of edible nanoemulsions: factors influencing droplet size produced by emulsion phase

inversion, J. Colloid Interface Sci. 388 (1) (2012) 95–102. https://doi.org/10.1016/j.jcis.2012.07.089.

[12] N. Gulati, H. Gupta, Parenteral Drug Delivery: A Review, DDF 5 (2) (2011) 133–145. https://doi.org/10.2174/187221111795471391.

[13] S. Baboota, F. Shakeel, A. Ahuja, J. Ali, S. Shafiq, Design, development and evaluation of novel nanoemulsion formulations for transdermal potential of celecoxib, Acta Pharm. 57 (3) (2007) 315–332. https://doi.org/10.2478/v10007-007-0025-5.

[14] S. Shafiq, F. Shakeel, S. Talegaonkar, F.J. Ahmad, R.K. Khar, M. Ali, Development and bioavailability assessment of ramipril nanoemulsion formulation, Eur. J. Pharm. Biopharm. 66 (2) (2007) 227–243. https://doi.org/10.1016/j.ejpb.2006.10.014.

[15] F. Shakeel, S. Baboota, A. Ahuja, J. Ali, M. Aqil, S. Shafiq, Nanoemulsions as vehicles for transdermal delivery of aceclofenac, AAPS PharmSciTech 8 (4) (2007) E104. https://doi.org/10.1208/pt0804104.

[16] T. Nakashima, M. Shimizu, M. Kukizaki, Membrane Emulsification by Microporous Glass, Key Eng Mater 61-62 (1992) 513–516. https://doi.org/10.4028/www.scientific.net/KEM.61-62.513.

[17] N.C. Christov, D. Ganchev, N.D. Vassileva, N.D. Denkov, K.D. Danov, P.A. Kralchevsky, Capillary mechanisms in membrane emulsification: oil-in-water emulsions stabilized by Tween 20 and milk proteins, Colloid Surface A 209 (1) (2002) 83–104. https://doi.org/10.1016/S0927-7757(02)00167-X.

[18] I. Kobayashi, M. Nakajima, S. Mukataka, Preparation characteristics of oil-in-water emulsions using differently charged surfactants in straight-through microchannel emulsification, Colloid Surface A 229 (1-3) (2003) 33–41. https://doi.org/10.1016/j.colsurfa.2003.08.005.

[19] F.A. Aguilar, B. Freudig, H.P. Schuchmann, Herstellen von Emulsionen in Hochdruckhomogenisatoren mit modifizierten Lochblenden, Chemie Ingenieur Technik 76 (4) (2004) 396–399. https://doi.org/10.1002/cite.200403375.

[20] I. Kobayashi, X. Lou, S. Mukataka, M. Nakajima, Preparation of monodisperse water-in-oil-in-water emulsions using microfluidization and straight-through microchannel emulsification, J Am Oil Chem Soc 82 (1) (2005) 65–71. https://doi.org/10.1007/s11746-005-1044-y.

[21] K. Köhler, F.A. Aguilar, A. Hensel, K. Schubert, H. Schubert, H.P. Schuchmann, Design of a Microstructured System for Homogenization of Dairy Products with High Fat Content, Chem Eng Technol 30 (11) (2007) 1590–1595. https://doi.org/10.1002/ceat.200700266.

[22] A. Baumann, S. Jeelani, B. Holenstein, P. Stössel, E.J. Windhab, Flow regimes and drop break-up in SMX and packed bed static mixers, Chemical Engineering Science 73 (2012) 354–365. https://doi.org/10.1016/j.ces.2012.02.006.

[23] K. Köhler, H.P. Schuchmann, Simultanes Emulgieren und Mischen, Chemie Ingenieur Technik 84 (9) (2012) 1538–1544. https://doi.org/10.1002/cite.201100095.

[24] P. Scholz, C.M. Keck, Nanoemulsions produced by rotor-stator high speed stirring, Int. J. Pharm. 482 (1-2) (2015) 110–117. https://doi.org/10.1016/j.ijpharm.2014.12.040.

[25] K. Shinoda, H. Arai, The Correlation between Phase Inversion Temperature In Emulsion and Cloud Point in Solution of Nonionic Emulsifier, J. Phys. Chem 68 (12) (1964) 3485–3490. https://doi.org/10.1021/j100794a007.

[26] C.W. Pouton, Formulation of self-emulsifying drug delivery systems, Advanced Drug Delivery Reviews 25 (1) (1997) 47–58. https://doi.org/10.1016/S0169-409X(96)00490-5.

[27] R.N. Gursoy, S. Benita, Self-emulsifying drug delivery systems (SEDDS) for improved oral delivery of lipophilic drugs, Biomed. Pharmacother. 58 (3) (2004) 173–182. https://doi.org/10.1016/j.biopha.2004.02.001.

[28] C. Bilbao-Sáinz, R.J. Avena-Bustillos, D.F. Wood, T.G. Williams, T.H. McHugh, Nanoemulsions Prepared by a Low-Energy Emulsification Method Applied to Edible Films, J Agric Food Chem 58 (22) (2010) 11932–11938. https://doi.org/10.1021/jf102341r.

[29] J. Schmidt, C. Damm, S. Romeis, W. Peukert, Formation of nanoemulsions in stirred media mills, Chemical Engineering Science 102 (2013) 300–308. https://doi.org/10.1016/j.ces.2013.08.018.

[30] A. Kwade, Determination of the most important grinding mechanism in stirred media mills by calculating stress intensity and stress number, Powder Technol 105 (1-3) (1999) 382–388. https://doi.org/10.1016/S0032-5910(99)00162-X.

[31] G.E. Granero, C. Ramachandran, G.L. Amidon, Dissolution and solubility behavior of fenofibrate in sodium lauryl sulfate solutions, Drug Dev. Ind. Pharm. 31 (9) (2005) 917–922. https://doi.org/10.1080/03639040500272108.

[32] T.J. Wooster, M. Golding, P. Sanguansri, Impact of oil type on nanoemulsion formation and Ostwald ripening stability, Langmuir 24 (22) (2008) 12758–12765. https://doi.org/10.1021/la801685v.

[33] G.I. Taylor, The Formation of Emulsions in Definable Fields of Flow, Proc R Soc A 146 (858) (1934) 501–523. https://doi.org/10.1098/rspa.1934.0169.

[34] S. Torza, R. Cox, S. Mason, Particle motions in sheared suspensions XXVII. Transient and steady deformation and burst of liquid drops, J. Colloid Interface Sci. 38 (2) (1972) 395–411. https://doi.org/10.1016/0021-9797(72)90255-X.

[35] B.J. Bentley, L.G. Leal, An experimental investigation of drop deformation and breakup in steady, two-dimensional linear flows, J. Fluid Mech. 167 (-1) (1986) 241. https://doi.org/10.1017/S0022112086002811.

[36] S. Fanselow, S.E. Emamjomeh, K.-E. Wirth, J. Schmidt, W. Peukert, Production of spherical wax and polyolefin microparticles by melt emulsification for additive manufacturing, Chemical Engineering Science 141 (2016) 282–292. https://doi.org/10.1016/j.ces.2015.11.019.

[37] F.v. Bruchhausen, G. Dannhardt, S. Ebel, A.-W. Frahm, E. Hackenthal, U. Holzgrabe (Eds.), Hagers Handbuch der pharmazeutischen Praxis, 5th ed., Springer, Berlin, Heidelberg, 1994.

[38] L.S. Wan, P.F. Lee, CMC of Polysorbates, Journal of Pharmaceutical Sciences 63 (1) (1974) 136–137. https://doi.org/10.1002/jps.2600630136.

[39] H.P. Karbstein, Untersuchungen zum Herstellen und Stabilisieren von Öl-in-Wasser-Emulsionen. phd thesis, Karlsruhe, 1994.

[40] M.H. Haque, A.R. Das, S.P. Moulik, Mixed Micelles of Sodium Deoxycholate and Polyoxyethylene Sorbitan Monooleate (Tween 80), J Colloid Interf Sci 217 (1) (1999) 1–7. https://doi.org/10.1006/jcis.1999.6267.

[41] M. Jumaa, B.W. Müller, The effect of oil components and homogenization conditions on the physicochemical properties and stability of parenteral fat emulsions, Int. J. Pharm. 163 (1-2) (1998) 81–89. https://doi.org/10.1016/S0378-5173(97)00369-4.

[42] B. Abismaïl, J. Canselier, A. Wilhelm, H. Delmas, C. Gourdon, Emulsification by ultrasound: Drop size distribution and stability, Ultrasonics Sonochemistry 6 (1-2) (1999) 75–83. https://doi.org/10.1016/S1350-4177(98)00027-3.

[43] S.Y. Tang, S. Manickam, T.K. Wei, B. Nashiru, Formulation development and optimization of a novel Cremophore EL-based nanoemulsion using ultrasound cavitation, Ultrasonics Sonochemistry 19 (2) (2012) 330–345. https://doi.org/10.1016/j.ultsonch.2011.07.001.

[44] J. Floury, A. Desrumaux, J. Lardières, Effect of high-pressure homogenization on droplet size distributions and rheological properties of model oil-in-water emulsions, Innovative Food Science & Emerging Technologies 1 (2) (2000) 127–134. https://doi.org/10.1016/S1466-8564(00)00012-6.

[45] S. Kentish, T.J. Wooster, M. Ashokkumar, S. Balachandran, R. Mawson, L. Simons, The use of ultrasonics for nanoemulsion preparation, Innovative Food Science & Emerging Technologies 9 (2) (2008) 170–175. https://doi.org/10.1016/j.ifset.2007.07.005.

[46] T.S.H. Leong, T.J. Wooster, S.E. Kentish, M. Ashokkumar, Minimising oil droplet size using ultrasonic emulsification, Ultrasonics Sonochemistry 16 (6) (2009) 721–727. https://doi.org/10.1016/j.ultsonch.2009.02.008.

[47] J.P. Guichard, P. Blouquin, Y. Qing, A New Formulation of Fenofibrate: Suprabioavailable Tablets, Current Medical Research and Opinion 16 (2) (2008) 134–138. https://doi.org/10.1185/0300799009117017.

[48] A. Avdeef, C.M. Berger, C. Brownell, pH-Metric Solubility. 2: Correlation Between the Acid-Base Titration and the Saturation Shake-Flask Solubility-pH Methods, Pharmaceutical Research 17 (1) (2000) 85–89. https://doi.org/10.1023/A:1007526826979.

[49] S.R. Vippagunta, Z. Wang, S. Hornung, S.L. Krill, Factors affecting the formation of eutectic solid dispersions and their dissolution behavior, Journal of Pharmaceutical Sciences 96 (2) (2007) 294–304. https://doi.org/10.1002/jps.20754.

[50] K. Pongsamart, P. Kleinebudde, S. Puttipipatkhachorn, Preparation of fenofibrate dry emulsion and dry suspension using octenyl succinic anhydride starch as emulsifying agent and solid carrier, Int. J. Pharm. 498 (1-2) (2016) 347–354. https://doi.org/10.1016/j.ijpharm.2015.12.041.

[51] A. Zaghloul, A.H. Nada, I. Khattab, Development, characterization and optimization of ibuprofen self-emulsifying drug delivery system applying face centered experimental design, Int. J. Pharmacy Tech. (3) (2011) 1674–1693.

**Supplementary Material**
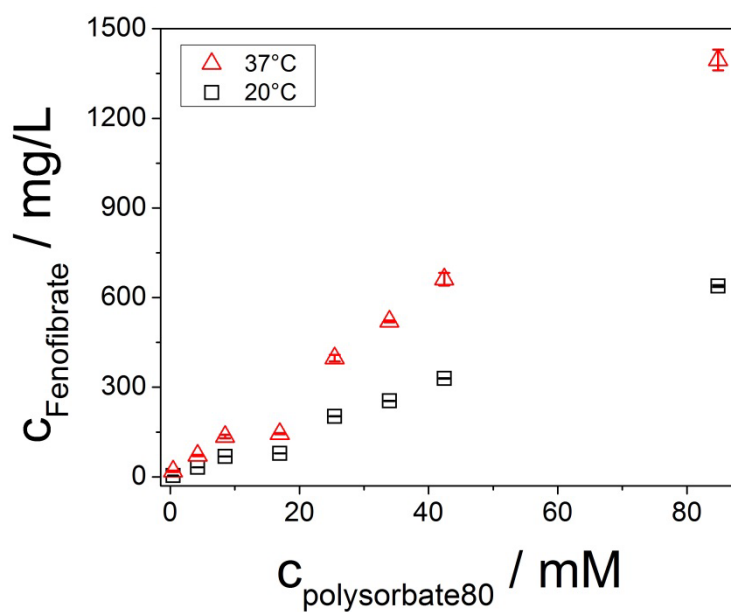


***Supplementary Figure S1*** *Influence of polysorbate 80 concentration and temperature on the aqueous solubility of fenofibrate.*